

# Dynamics of Field Induced Polarization Reversal in Strained Perovskite Ferroelectric Films with c-oriented Polarization

Laurent Baudry,<sup>1,\*</sup> Igor A. Luk'yanchuk,<sup>2,3</sup> and Anna Razumnaya<sup>4</sup>

<sup>1</sup>*Institute of Electronics, Microelectronics and Nanotechnology (IEMN)-DHS Département, UMR CNRS 8520, Université des Sciences et Technologies de Lille, 59652 Villeneuve d'Ascq Cedex, France*

<sup>2</sup>*Laboratory of Condensed Matter Physics, University of Picardie Jules Verne, Amiens, 80039, France*

<sup>3</sup>*L. D. Landau Institute for Theoretical Physics, Moscow, Russia*

<sup>4</sup>*Physics Department, Southern Federal University, Rostov on Don, 344090 Russia*

(Dated: February 17, 2019)

The field-induced polarization reversal in *c*-oriented ferroelectric phase of strained perovskite film has been studied. We show that in addition to the conventional longitudinal switching mechanism, when *c*-oriented polarization vector changes its modulus, the longitudinal-transversal and transversal mechanisms when the perpendicular component of polarization is dynamically admixed are possible. The later process can occur either via the straight-abrupt or initially-continuous polarization turnover scenario. We specified the obtained results for the case of PbTiO<sub>3</sub> and BaTiO<sub>3</sub> ferroelectrics and propose the experimental methods for their investigation.

Dynamical switching properties of ferroelectrics are essential for their application in the memory-storage devices [1]. The underlying mechanism of polarization reversal is of special interest for the mostly used pseudocubic perovskite crystals that, depending on the orientation of polarization  $\mathbf{P} = (P_1, P_2, P_3)$  can exhibit tetragonal, orthorhombic or rhombohedral structural phases in the ferroelectric state of the bulk material [2]. The situation is more diverse in case of substrate-deposited perovskite ferroelectric films in which the substrate-provided deformation makes the lattice constant *c* in *z*-direction (perpendicular to the film surface) different from the in-plane lattice constants  $a = b$  already in the high-temperature paraelectric phase with  $\mathbf{P} = 0$ . In particular, Pertsev, Zembilgotov and Tagantsev [3, 4] studied the effect of substrate clamping on PbTiO<sub>3</sub> and BaTiO<sub>3</sub> films and proposed that at least four structural phases can exist in strain-temperature,  $u_m$ -*T* phase diagram (Fig. 1). The so-called *c*-phase with  $\mathbf{P} = (0, 0, P_3)$  occurs at high compressive strains whereas the *aa*-phase with  $\mathbf{P} = (P_1, P_1, 0)$  is realized at high tensile strains. Either *ac*-phase with  $\mathbf{P} = (P_1, 0, P_3)$  or *r*-phase with  $\mathbf{P} = (P_1, P_1, P_3)$  can occur at low strains. These phases are thermodynamically stable and separated by continuous (thin) or discontinuous (bold) transition lines in Fig. 1.

In the present letter we study polarization switching in PbTiO<sub>3</sub> and BaTiO<sub>3</sub> oxides induced by the applied electric field and demonstrate that the situation is even more rich. Additional phases can dynamically appear during the polarization reversal. We restrict ourselves to the *c*-phase region of  $u_m$ -*T* phase diagram and consider the switching process when the initially up-oriented polarization  $\mathbf{P} = (0, 0, P_3)$  decreases and then suddenly drops down under the oppositely applied field  $\mathbf{E} = (0, 0, E)$  with  $E < 0$ .

To describe the PbTiO<sub>3</sub> and BaTiO<sub>3</sub> materials we use the renormalized Landau-Devonshire functional given in

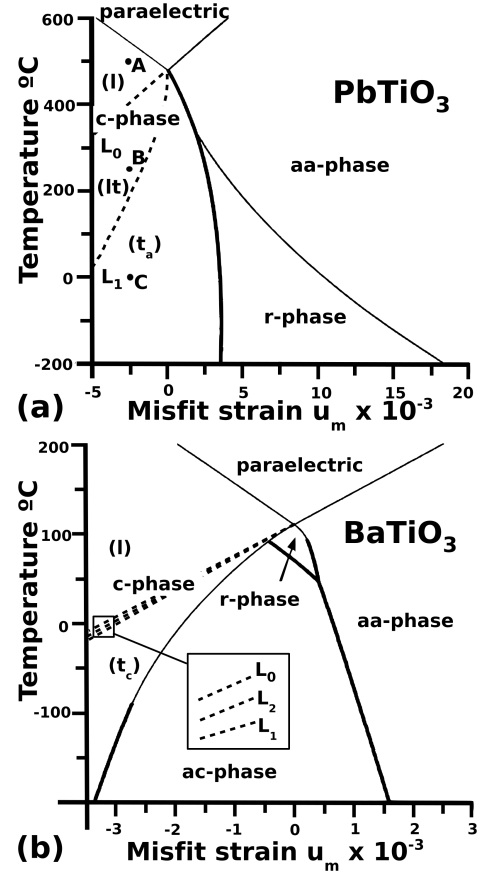


FIG. 1. Regions of the longitudinal (*l*), longitudinal-transversal (*lt*) and transversal (*t*) switching regimes and corresponding separating lines  $L_0$  and  $L_1$  on the phase diagrams of strained films of PbTiO<sub>3</sub> (a) and BaTiO<sub>3</sub> (b), adopted from Ref. [3]. Stability line  $L_2$  determines the type of transversal switching. Close location of  $L_2$  and  $L_1$  for BaTiO<sub>3</sub> implies that it occurs according the initially-continuous turnover of polarization ( $t_c$ ), whereas the absence of this line for PbTiO<sub>3</sub> means that transversal switching is straight-abrupt ( $t_a$ )

[3], for which the account of the six-order terms is known to be important [5–7]:

The last term in Eq. (1) presents the field-driving interaction with electric polarization. The renormalized coefficients  $a_1^*$ ,  $a_3^*$ ,  $a_{11}^*$ ,  $a_{33}^*$ ,  $a_{13}^*$  and  $a_{12}^*$  depend on the misfit strain  $u_m$  and temperature  $T$  whereas other coefficients  $s_{11}$ ,  $s_{12}$ ,  $a_{111}$ ,  $a_{112}$  and  $a_{123}$  correspond to its bulk homologous, as was explicitly specified in Ref. [3].

$$\begin{aligned} \tilde{G}(\mathbf{P}, E, T, u_m) = & a_1^* (P_1^2 + P_2^2) + a_3^* P_3^2 + a_{11}^* (P_1^4 + P_2^4) \\ & + a_{33}^* P_3^4 + a_{13}^* (P_1^2 + P_2^2) P_3^2 + a_{12}^* P_1^2 P_2^2 + a_{123} P_1^2 P_2^2 P_3^2 \\ & + a_{112} [P_1^4 (P_2^2 + P_3^2) + P_3^4 (P_1^2 + P_2^2) + P_2^4 (P_1^2 + P_3^2)] \\ & + a_{111} (P_1^6 + P_2^6 + P_3^6) + \frac{u_m^2}{s_{11} + s_{12}} - EP_3. \end{aligned} \quad (1)$$

Note that several alternative approaches were proposed to establish the  $u_m$ - $T$  phase diagram of BaTiO<sub>3</sub> [8–10]. Their results are competitive with [3, 4] mostly in relative location of  $r$ - and  $ac$ - phases. This minor difference is not essential for our consideration and can be easily taken into account for each particular case. In what follows, we consider the competition between the switching-induced  $ac$  and  $r$  phases. By substitution of the corresponding order parameters  $\mathbf{P} = (P_1, 0, P_3)$  and  $\mathbf{P} = (P_1, P_1, P_3)$  in (1) we obtain the following effective functional:

$$\begin{aligned} \tilde{G} = & \frac{b_1}{2} P_1^2 + \frac{b_3}{2} P_3^2 + \frac{b_{11}}{4} P_1^4 + \frac{b_{33}}{4} P_3^4 + \frac{b_{13}}{2} P_1^2 P_3^2 \quad (2) \\ & + \frac{b_{113}}{2} P_1^4 P_3^2 + \frac{b_{133}}{2} P_1^2 P_3^4 + \frac{b_{111}}{6} P_1^6 + \frac{b_{333}}{6} P_3^6 - EP_3, \end{aligned}$$

where  $b_1 = 2a_1^*$ ,  $b_3 = 2a_3^*$ ,  $b_{11} = 4a_{11}^*$ ,  $b_{13} = 2a_{13}^*$ ,  $b_{33} = 4a_{33}^*$ ,  $b_{111} = 6a_{111}^*$ ,  $b_{113} = 2a_{112}^*$ ,  $b_{133} = 2a_{112}^*$ ,  $b_{333} = 6a_{111}^*$  for  $ac$ -phase case and  $b_1 = 2a_1^*$ ,  $b_3 = 2a_3^*$ ,  $b_{11} = 8a_{11}^* + 2a_{12}^*$ ,  $b_{13} = 4a_{13}^*$ ,  $b_{33} = 4a_{33}^*$ ,  $b_{111} = 12a_{111}^* + 12a_{112}^*$ ,  $b_{113} = 2a_{123}^* + 4a_{112}^*$ ,  $b_{133} = 4a_{112}^*$ ,  $b_{333} = 6a_{111}^*$  for  $r$ -phase case.

Our approach is inspired by that given by Iwata and Ishibashi [11] for the case of cubic (unstrained) lattice in paraelectric phase. It was demonstrated that depending on the strength of the polarization-lattice coupling, two reversal mechanisms are possible. For strong cubic anisotropy the switching occurs like in uniaxial one-component ferroelectrics by dynamical change of the modulus of the longitudinal polarization component  $P_3$ . For weak anisotropy the transversal component  $P_1$  virtually admixes to  $P_3$  during the process. Such *polarization-rotation* scenario can, for instance, occurs in PbZr<sub>x</sub>Ti<sub>1-x</sub>O<sub>3</sub> compounds when the anisotropic coupling is soften just as the composition parameter  $x$  approaches the morphotropic point  $x \simeq 0.44$  from above.

The distinguishing feature of the substrate-deposited films from the bulk cubic case is the strain-induced uniaxial anisotropy that is reflected both by the splitting of the critical temperatures in the second order  $P_1^2$  and  $P_3^2$

terms and by accounting for the 6th-order cross-coupling terms. To understand the dynamical mechanism of polarization reversal we should catch the critical field at which the switching instability occurs. Application of an opposite electric field leads to the decrease of  $c$ -oriented polarization which stays yet positive until the critical field is reached. At this stage the field-driven polarization evolution,  $P_3(E)$  is given by the one-component variational equation:

$$\left( \frac{\partial \tilde{G}}{\partial P_3} \right)_{P_{1,2}=0} = b_3 P_3 + b_{33} P_3^3 + b_{333} P_3^5 - E = 0. \quad (3)$$

The value of the critical field at which polarization switching starts can be obtained from the loss of the positive definiteness of the Hessian matrix  $H_{ij} = \frac{\partial^2 \tilde{G}}{\partial P_i \partial P_j}$ , presented in the extremal point of initial equilibrium  $P_1 = 0$ ,  $P_3 = P_3(E)$  as:

$$H_{33} = b_3 + 3b_{33} P_3^2 + 5b_{333} P_3^4, \quad (4)$$

$$H_{11} = b_1 + b_{13} P_3^2 + b_{133} P_3^4, \quad (5)$$

$$H_{13} = H_{31} = 0. \quad (6)$$

where the dependence  $P_3(E)$  is given by Eq.(3). Upon field increase the competition occurs between the longitudinal and transversal critical fields  $E^{(l)}$  and  $E^{(t)}$ , determined by the conditions  $H_{33}(P_3(E^{(l)})) = 0$  and  $H_{11}(P_3(E^{(t)})) = 0$ . Importantly, the switching occurs at the instability field  $E^{(l)}$  or  $E^{(t)}$  which is attained first and the further scenario of polarization vector evolution is determined by the occurring type of instability.

(i) For  $|E^{(l)}| < |E^{(t)}|$  the *longitudinal* ( $l$ ) switching instability is realized first and the polarization vector reverses its direction by change of the amplitude of  $P_3$  from positive to negative, passing through  $P_3 = 0$ .

(ii) For  $|E^{(t)}| < |E^{(l)}|$  the *transversal* ( $t$ ) switching instability is realized first and the component  $P_1$  is admixed to  $P_3$  after the beginning of the reversal process, just above  $E^{(t)}$ . Polarization switching has therefore the rotational constituent, like in the Iwata and Ishibashi model.

(iii) There can exist also the mixed *longitudinal-transversal* ( $lt$ ) regime when the polarization reversal starts according to longitudinal scenario at  $E = E^{(l)}$  but the transversal component  $P_1$  virtually appears at the later stage of the process.

The polarization evolution in  $l$ ,  $lt$  and  $t$  switching regimes is sketched in Fig. 2. We presume that they are separated by crossover lines  $L_0$  and  $L_1$  in  $u_m$ - $T$  phase diagram and find the condition of their existence. The  $t$ -type switching can have either initially continuous ( $t_c$ ) or straight-abrupt ( $t_a$ ) character as will be specified later.

According to the given above consideration the transversal component  $P_1$  can dynamically admix to the component  $P_3$  during polarization reversal if the

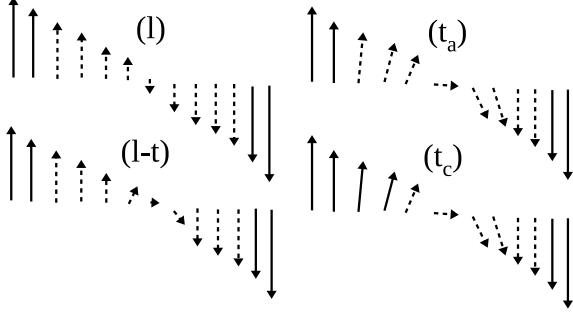


FIG. 2. Reversal of the polarization vector as function of increasing with time switching electric field during longitudinal ( $l$ ), longitudinal-transversal ( $lt$ ), transversal straight-abrupt ( $t_a$ ) and transversal initially-continuous ( $t_c$ ) switching. Solid lines present the thermodynamically stable field-induced states whereas the dashed lines present the dynamically-virtual states during the abrupt switching process.

polarization-dependent Hessian matrix element  $H_{11}$  becomes negative in course of the switching. This occurs e.g., when coefficient  $b_1$  is negative. If the dropping-down polarization goes through the state with vanishing  $P_3$ , the element  $H_{11}$ , according to Eq. (5) acquires the negative sign in the vicinity of  $P_3 = 0$ . The polarization vector will experience the instability towards the transversal deviation and the  $lt$  regime will be realized. Therefore the crossover line  $L_0$  between  $l$  and  $lt$  regimes is given by the condition:

$$L_0 : b_1(u_m, T) = 0. \quad (7)$$

Noteworthy that the line  $L_0$  can be found in  $u_m$ - $T$  phase diagram as the prolongation of the paraelectric- $aa$  phase transition line located in  $u_m > 0$  region into the  $u_m < 0$  region.

The condition of crossover between  $lt$  and  $t$  switching regimes can be found by equating the critical fields  $E^{(l)}$  and  $E^{(t)}$  or, what is equivalent and easier, by equating the corresponding longitudinal and transversal critical polarizations  $P_3^{(l)} = P_3(E^{(l)})$ ,  $P_3^{(t)} = P_3(E^{(t)})$  calculated at these fields. The latter can be found from Eqs.  $H_{33}(P_3^{(l)}) = 0$  and  $H_{33}(P_3^{(t)}) = 0$  as:

$$P_3^{(l)2} = \frac{(9b_{33}^2 - 20b_3b_{333})^{1/2} - 3b_{33}}{10b_{333}}, \quad (8)$$

$$P_3^{(t)2} = \frac{(b_{13}^2 - 4b_1b_{133})^{1/2} - b_{13}}{2b_{133}}. \quad (9)$$

Condition  $P_3^{(l)} = P_3^{(t)}$  determines the crossover line  $L_1$  between  $lt$  and  $t$  regimes:

$$L_1: \frac{b_3b_{13} - 3b_1b_{33}}{5b_1b_{333} - b_3b_{133}} = \frac{5b_1b_{333} - b_3b_{133}}{3b_{33}b_{133} - 5b_{13}b_{333}}. \quad (10)$$

To be more specific we delimit the location of  $l$ ,  $lt$  and  $t$  switching regimes and corresponding crossover lines  $L_0$

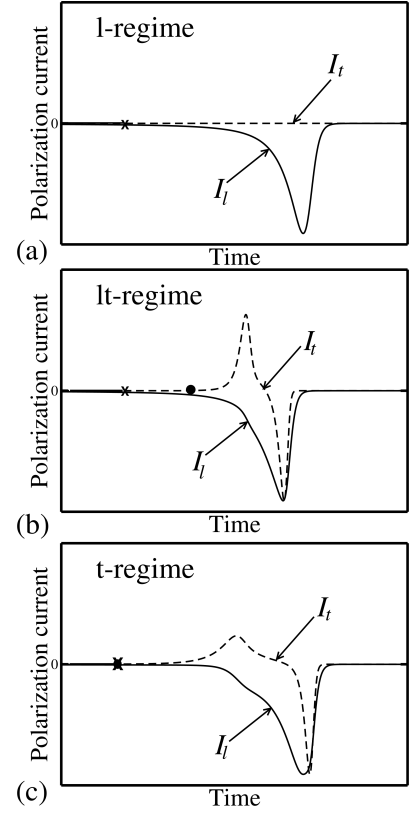


FIG. 3. Time dependence of the longitudinal,  $I_l = \frac{dP_3}{dt}$  and transversal,  $I_t = \frac{dP_1}{dt}$  polarization currents for (a) transversal ( $t$ ), (b) longitudinal-transversal ( $lt$ ) and (c) longitudinal ( $l$ ) switching regimes for  $\text{PbTiO}_3$ . Panels (a), (b) and (c) correspond to the points A, B and C in Fig. 1 (a). The cross and circle markers indicate the beginning of the longitudinal and transversal polarization reversal process correspondingly.

and  $L_1$  on phase diagram of strained  $\text{PbTiO}_3$  and  $\text{BaTiO}_3$  films using the appropriate strain and temperature dependencies of coefficients of functional (2) and examining separately the cases of transitions through the  $ac$  and  $r$  phases.

In the case of  $\text{PbTiO}_3$  all these regimes are clearly visible and are located inside the region of thermodynamically stable  $c$ -phase as shown in Fig. 1 (a). To study the transient polarization dynamics we select the representative points for each transition region (points A, B and C in Fig. 1 (a)) and numerically solve the Landau-Khalatnikov kinetic equations.

$$L_i \frac{dP_i}{dt} = -\frac{\delta \tilde{G}}{\delta P_i}, \quad (11)$$

for each polarization component  $P_i = P_i(t)$ . Here  $L_i$  are the corresponding damping coefficients. The results are presented in Fig. 3 in form of experimentally measurable longitudinal and transversal polarization currents  $I_l = \frac{dP_3}{dt}$  and  $I_t = \frac{dP_1}{dt}$ .

Point A is selected for the  $l$ -switching region at  $u_m = -0.0025$  and  $T = 500^\circ\text{C}$ . As it follows from Fig. 3 (a)

the polarization current has only the longitudinal component that is characteristic for the longitudinal switching regime. Point B corresponds to the  $lt$ -switching region and is taken at  $u_m = -0.0025$ ,  $T = 250^\circ\text{C}$ . As shown in Fig. 3 (b) both components of polarization current are observed but the transversal one is excited after the longitudinal one and vanishes earlier than the longitudinal one. Point C is taken in the  $t$ -switching region at  $u_m = -0.0025$  and  $T = 0^\circ\text{C}$ . As shown in Fig. 3 (c) the longitudinal and transversal polarization currents are excited simultaneously.

In the case of  $\text{BaTiO}_3$  [Fig. 1 (b)] one can observe only the  $l$  and  $t$ -switching regimes. The  $lt$ -switching regime is difficult to detect because of the very close location of the lines  $L_0$  and  $L_1$ .

An important issue for the  $t$ -type switching is the dynamical behavior of polarization just upon reaching the transversal instability field. Under certain conditions the intermediately-stable  $ac$ - or  $r$ - phase can be induced just above  $E^{(t)}$ . Then, the continuous (as function of the field) turnover of polarization through this phase will precede the abrupt rotational drop-down. To distinguish between the shown in Fig. 2 initially-continuous ( $t_c$ ) and straight-abrupt ( $t_a$ ) transversal switching process we study the global stability of functional (2) with respect to small deviations  $\Delta P_1$ ,  $\Delta P_3$  about the equilibrium point  $P_1^{(t)} = 0$  and  $P_3^{(t)} = P_3(E^{(t)})$  exactly at  $E = E^{(t)}$ . This is a peculiar problem since at  $E = E^{(t)}$  the coefficient  $H_{11}$  before  $(\Delta P_1)^2$  is equal to zero and the higher-order terms should be taken into account. Following the catastrophe theory we keep only the most relevant terms and present the expansion of (2) as:

$$\tilde{G} \approx \frac{1}{2}\rho(\Delta P_3)^2 + \mu(\Delta P_3)(\Delta P_1)^2 + \frac{1}{2}\lambda(\Delta P_1)^4, \quad (12)$$

where  $\rho = H_{33}$  (see (5)),  $\mu = \frac{1}{2}\frac{\partial^3 \tilde{G}}{\partial P_3 \partial P_1^2} = b_{13}P_3^{(t)} + 2b_{133}P_3^{(t)3}$  and  $\lambda = \frac{1}{12}\frac{\partial^4 \tilde{G}}{\partial P_1^4} = \frac{1}{2}b_{33}$ . Transformation  $x = (\Delta P_1)^2$  and  $z = (\Delta P_3)$  maps the problem onto the study of quadratic functional  $\frac{1}{2}\lambda x^2 + \mu xy + \frac{1}{2}\rho y^2$ . The last one is globally unstable at  $\lambda\rho > \mu^2$  that provides the straight-abrupt switching at  $E \gtrsim E^{(t)}$ . At  $\lambda\rho < \mu^2$  this functional is locally stable and at the initial stage of reversal process the  $P_1$  component develops continuously as a function of the field. Using the given above definition of  $\lambda$ ,  $\rho$ ,  $\mu$  and excluding  $P_3^{(t)}$  according Eq. (9) we, after some algebra, present the line  $L_2$ , separating these two regimes on the  $u_m$ - $T$  phase diagram by equation:

$$L_2: \quad PR = Q^2. \quad (13)$$

with

$$\begin{aligned} P &= b_3b_{33}b_{13} - 3b_1b_{33}^2 + 2b_1b_{13}^2 - 8b_1^2b_{133}, \\ Q &= 5b_1b_{33}b_{333} - b_3b_{33}b_{133}, \\ R &= 3b_{33}^2b_{133} - 2b_{13}^2b_{133} + 8b_1b_{13}^2 - 5b_{13}b_{33}b_{333}. \end{aligned} \quad (14)$$

The  $t_c$  and  $t_a$  switching regions being located below and above this line correspondingly.

Thoughtful analysis of equation (13) for  $\text{BaTiO}_3$  case shows that the line  $L_2$  is located very close to the line  $L_1$  (see Fig. 1 b) which means that  $t_c$ -type of the switching always occurs through the intermediate field-induced  $ac$ -phase. In contrast, the line  $L_2$  does not exist in  $c$ -phase region of the phase diagram of  $\text{PbTiO}_3$  [Fig. 1 (a)] which implies the  $t_a$ -type of the switching through the intermediate  $r$ -phase.

In this letter we have demonstrated the existence of different polarization reversal regimes in strained pseudocubic ferroelectric  $\text{PbTiO}_3$  and  $\text{BaTiO}_3$  films. Depending on the temperature and on the misfit strain one can distinguish the polarization reversal governed by the longitudinal, transversal or mixed longitudinal-transversal switching regimes. All three mechanisms can be observed in  $\text{PbTiO}_3$  compounds. In  $\text{BaTiO}_3$  compounds only the longitudinal and transversal mechanisms can be detected. The later occurs through the intermediate  $ac$ -phase with initial continuous turnover of the polarization vector as function of the field. The dynamic appearance of the transversal polarization during transition can be observed by the time-resolved piezo-force microscopy or by the in-field Raman spectroscopy sensitive to the polarization vector variation. Note, however that situation can be even more complex if the  $180^\circ$  ferroelectric domains exist in the initial  $c$ -phase or/and  $90^\circ$  transversal ferroelastic domains emerge during the switching process. The study of such scenarios can be done on the basis of presented above calculations.

This work was supported by FP7 ITN-NOTEDDEV and IRSES-SIMTECH MC mobility programs.

---

\* laurent.baudry@iemn.univ-lille1.fr

- [1] J. F. Scott, *Ferroelectric Memories*, Advanced microelectronics, Springer, 2000.
- [2] M. E. Lines and A. M. Glass, *Principles and Applications of Ferroelectrics and Related Materials*, Oxford University Press, 1977.
- [3] N. A. Pertsev, A. G. Zembilgotov, and A. K. Tagantsev, *Phys. Rev. Lett.* **80**, 1988 (1998).
- [4] N. A. Pertsev, A. G. Zembilgotov, and A. K. Tagantsev, *Ferroelectrics* **223**, 78 (1999).
- [5] A. J. Bell and L. E. Cross, *Ferroelectrics* **59**, 197 (1984).
- [6] Y. L. Li, L. E. Cross, and L. Q. Chen, *J. Appl. Phys.* **98**, 064101 (2005).
- [7] Y. L. Wang et al., *J. Appl. Phys.* **101**, 104115 (2007).
- [8] O. Diéguez et al., *Phys. Rev. B* **69**, 212101 (2004).
- [9] B.-K. Lai, I. A. Kornev, L. Bellaiche, and G. J. Salamo, *Applied Physics Letters* **86**, (2005).
- [10] V. B. Shirokov, Yu. I. Yuzyuk, B. Dkhil and V. V. Lemanov *Phys. Rev. B* **75**, 224116 (2007)
- [11] M. Iwata and Y. Ishibashi, *Jpn. J. Appl. Phys.* **38**, 5670 (1999).